
THE DEVELOPMENT OF A DENOISING MODEL FOR LODOX[®] STATSCAN[®] IMAGES

A Phantom Study



UNIVERSITY OF CAPE TOWN
DEPT. OF ELECTRICAL ENGINEERING

Presented by:

Travimadox Webb

Prepared for:

Dr. Yaaseen Martin(Supervisor)

Dr. Lindie Du Plessis(Co-supervisor)

September 12, 2024

Submitted to the Department of Electrical Engineering at the University of Cape Town in partial fulfilment of the academic requirements for the degree of Bachelor of Science degree in Electrical and Computer Engineering.

Abstract

In this work we describe a novel Thesis Template, to be used by students in Electrical & Engineering at the University of Cape Town. This section entails the abstract of the document.

Coming soon

Acknowledgments

I would like to thank The MasterCard Foundation for funding my four-year undergrad degree, enabling me to achieve my lifelong dream of becoming an engineer. With their financial support and mentorship, I have been able to achieve this dream.

Words cannot express my gratitude to my supervisor, Dr. Yaaseen, for his invaluable patience and feedback on Machine Learning and Digital Signal Processing techniques for image processing. I also could not have undertaken this journey without my co-supervisor, Dr Lindie, who generously provided knowledge and expertise in Medical Imaging Technologies to enable me to complete this thesis successfully.

I am also grateful to my classmates and cohort members, especially my friends Clifford and Thikazi, for their constant emotional support, late-night feedback sessions, and moral support. Thanks should also go to the biomedical lab technical officer from the university, who guided me closely in learning how to use the Lodox technology.

Lastly, I would be remiss in not mentioning my family, especially my parents, Daniel and Violet, and siblings, namely Carlsberg, Bevy and Brasil. Their belief in me has kept my spirits and motivation high during this process.

Declaration

1. I know that plagiarism is wrong. Plagiarism is to use another's work and pretend that it is one's own.
2. I have used **IEEE** for citation and referencing. Each contribution to, and quotation in, this report from the work(s) of other people has been attributed, and has been cited and referenced.
3. This report is my own work, and is in my own words except where I have used quotations.
4. I have not paid a third party to complete my work on my behalf. My use of artificial intelligence software has been limited to **grammar mistakes correction, cohesion and clarity suggestions**.
5. I have not allowed and will not allow anyone to copy my work with the intention of passing it off as his or her own work.
6. I acknowledge that copying someone else's assignment or essay, or part of it, is wrong, and declare that this is my own work.

900

Word count

T·C·W

Travimadox Webb

September 12, 2024

Glossary

Anscombe transform A variance-stabilizing transformation used to approximate the distribution of Poisson-distributed data by a normal distribution, often applied in image processing and statistics.. [9](#), [13](#), [15](#)

FBPconvNet A convolutional neural network architecture designed for improving image reconstruction in CT scans. It builds upon the traditional Filtered Back Projection (FBP) method by introducing convolutional layers that enhance image quality, particularly in low-dose CT images. FBPconvNet focuses on reducing artifacts and noise while preserving essential image details.. [20](#)

FBPTransNet A neural network architecture that enhances image quality in CT scans by replacing the maximum pooling layers of FBPconvNet with Transformer modules. FBPTransNet features dual inlets and outlets to simultaneously process high and low energy CT images, and employs a multi-head attention mechanism to effectively model noise maps and recover fine texture details in the denoised images.. [20](#)

golden hour term often used in trauma or emergency care to suggest that an injured or sick person must receive definitive treatment within the first 60 minutes from the time of injury or appearance of symptoms. [1](#)

Staircase effect An artifact in digital imaging where smooth gradations of intensity are represented by abrupt steps or bands, rather than a continuous transition. This effect is commonly observed in images with low bit depth or when using inadequate interpolation methods.. [10](#)

U-Net A type of convolutional neural network architecture primarily used for image segmentation tasks. It consists of an encoder-decoder structure with skip connections, enabling precise localisation and efficient learning from limited data. U-Net is widely used in medical image analysis due to its ability to produce accurate segmentation even with small training datasets.. [19](#), [20](#)

Yaroslavsky filter A type of neighbourhood filter used in image processing for denoising images. It averages pixel values in a neighborhood but only includes those with similar intensity to the central pixel, effectively reducing noise while preserving edges. This method is computationally efficient and commonly used in fields like medical imaging and photography.. [16](#)

Acronyms

- ADF** Anisotropic Diffusion Filter. [10](#)
- ASIC** application-specific integrated circuits. [6](#)
- ASO** Atom Search Optimization. [13](#)
- ATV** Adaptive Total Variation method. [11](#)
- AWGN** Additive White Gaussian Noise. [7](#), [9](#)
- BF** Bilateral Filter. [10](#), [13](#)
- BM3D** Block Matching and 3D filtering. [13–18](#), [20](#)
- BRISQUE** Blind/Referenceless Image Spatial Quality Evaluator. [12](#)
- CCD** Charge Coupled Detector. [1](#), [8](#)
- CNN** Convolutional Neural Networks. [17](#), [19](#), [20](#)
- CNR** Contrast to Noise Ratio. [12](#)
- COV** Coefficient of Variation. [12](#)
- CT** Computed Tomography. [1](#), [2](#), [19](#), [20](#)
- DnCNN** denoising convolutional neural networks. [18](#)
- DSP** Digital Signal Processing. [10](#), [20](#)
- DTCWT** dual tree complex wavelet transform. [13](#), [14](#)
- FIR** finite impulse response. [13](#)
- FNLM** Fast Non-Local Means. [11](#), [12](#)
- GPU** Graphical Processing Unit. [17](#)

HNIPM Hybrid Non-iterative Poisson Model. [15](#)

IBS improved threshold shrinkage. [14](#)

ICA Independent Component Analysis. [16](#)

LPA-RICI Local Polynomial Approximation - Relative Intersection of Confidence Intervals. [16](#)

ML Machine Learning. [17](#), [20](#)

MMI Multiscale Multiplicative Innovations. [13](#)

MRI Magnetic Resonance Imaging. [20](#)

MROF Modified Rudin-Osher-Fatemi model. [11](#)

MS-VST multiscale variance stabilizing transform. [13](#), [15](#)

MSE Mean Squared Error. [12](#), [13](#)

N2N Noise2Noise. [17](#), [18](#), [20](#)

N2V Noise2Void. [17](#), [18](#), [20](#)

NIQE Natural Image Quality Evaluator. [12](#)

NLM Non-Local Means. [xiii](#), [11–13](#), [15](#), [16](#), [20](#)

NNPS Normalized Noise Power Spectrum. [12](#)

PCA Principal Component Analysis. [15](#), [17](#)

PCCT Photon-counting CT. [15](#)

PCD Photon Counting Detector. [1](#), [2](#), [6](#), [8](#), [19](#)

PKAID-Net prior knowledge-aware iterative denoising neural network. [19](#)

PRBF Poisson Reducing Bilateral Filter. [10](#)

PSNR Peak Signal-to-Noise Ratio. [18](#)

PURE-LET Poisson Unbiased Risk Estimation – Linear Expansion of Thresholds. [13](#)

R-L Richardson-Lucy algorithm. [11](#)

ROF Rudin-Osher-Fatemi model. [10](#), [11](#)

TV Total Variation. [xiii](#), [10](#), [11](#), [19](#), [20](#)

UV Ultraviolet rays. [5](#)

VMI Virtual Monoenergetic Images. [19](#)

VST Variance Stabilising Transform. [9](#)

WNNM Weighted nuclear norm minimization. [18](#)

Contents

Abstract	ii
Acknowledgments	iii
Declaration	iv
Glossary	v
Acronyms	vii
Table of Contents	x
List of Figures	xii
List of Tables	xiii
List of Equations	xiv
Nomenclature	xv
Chapter 1: Introduction	1
1.1 Background	1
1.2 Motivation	2
1.3 Problem Statement	2
1.4 Objectives	2
1.5 Contributions	3
1.6 Scope and Limitations	3
1.7 Outline	3
Chapter 2: Literature Review	4
2.1 X-ray Imaging Fundamentals	4
2.1.1 X-ray Production	4
2.1.2 X-ray Attenuation	5
2.1.3 X-ray Detection and Image Formation	5

2.2	Noise in X-ray imaging	6
2.2.1	Types of Noise in X-ray Imaging	6
2.2.2	Impact of Noise on Image Quality and Diagnosis	8
2.3	Denoising	8
2.3.1	Classical Filters	10
2.3.2	Hybrid Filters	14
2.3.3	Deep Learning Methods	17
2.4	Conclusion	20
Chapter 3:	Methodology	21
Chapter 4:	Design	22
Chapter 5:	Results	23
Chapter 6:	Conclusions	24
	Bibliography	25
	Appendix A: Supporting Data	33
	Appendix B: Satirical Support	34

List of Figures

2.1 Diagram illustrating the generation of quantum noise in X-ray imaging due to the uneven distribution of X-ray photons on the PCD detector surface, resulting in a noisy image output. Created with BioRender.com 7

List of Tables

2.1	Summary of Photon Interaction Mechanisms and Their Significance in Medical Imaging.	5
2.2	Summary of Adaptations to Total Variation (TV) Filters to addressing challenges in original TV filter.	11
2.3	Summary of Proposed Solutions to Address Challenges in Non-Local Means (NLM) Filter	12
2.4	Summary of Wavelet Filter Variations for Poisson Noise Reduction in Medical and X-ray Images, Highlighting Strengths and Challenges	14
2.5	Summary of Hybrid Filters for X-ray Image Denoising	16
2.6	Summary of Deep Learning Approaches for X-Ray Image Denoising	20

List of Equations

Nomenclature

Anscombe transform A variance-stabilizing transformation used to approximate the distribution of Poisson-distributed data by a normal distribution, often applied in image processing and statistics.. [9](#), [13](#), [15](#)

FBPconvNet A convolutional neural network architecture designed for improving image reconstruction in CT scans. It builds upon the traditional Filtered Back Projection (FBP) method by introducing convolutional layers that enhance image quality, particularly in low-dose CT images. FBPconvNet focuses on reducing artifacts and noise while preserving essential image details.. [20](#)

FBPTransNet A neural network architecture that enhances image quality in CT scans by replacing the maximum pooling layers of FBPconvNet with Transformer modules. FBPTransNet features dual inlets and outlets to simultaneously process high and low energy CT images, and employs a multi-head attention mechanism to effectively model noise maps and recover fine texture details in the denoised images.. [20](#)

golden hour term often used in trauma or emergency care to suggest that an injured or sick person must receive definitive treatment within the first 60 minutes from the time of injury or appearance of symptoms. [1](#)

Staircase effect An artifact in digital imaging where smooth gradations of intensity are represented by abrupt steps or bands, rather than a continuous transition. This effect is commonly observed in images with low bit depth or when using inadequate interpolation methods.. [10](#)

U-Net A type of convolutional neural network architecture primarily used for image segmentation tasks. It consists of an encoder-decoder structure with skip connections, enabling precise localisation and efficient learning from limited data. U-Net is widely used in medical image analysis due to its ability to produce accurate segmentation even with small training datasets.. [19](#), [20](#)

Yaroslavsky filter A type of neighbourhood filter used in image processing for denoising images. It averages pixel values in a neighborhood but only includes those with similar intensity to the central pixel, effectively reducing noise while preserving edges. This method is computationally efficient and commonly used in fields like medical imaging and photography.. [16](#)

Chapter 1

Introduction

1.1 Background

Timely and accurate diagnosis is a critical feature of trauma care as it directly impacts patients survival. Studies have shown that accurate information acquired during the [golden hour](#) is essential to saving patients' lives in trauma centres [1], [2]. One of the most important diagnostic tools in trauma care is medical imaging as it allows healthcare professionals to visualise internal body structures non-invasively. This gives accurate information on the extent of injuries enabling them to develop an effective prioritisation plan for the treatment phase. Among the many medical imaging technologies, X-ray remains one of the most widely used due to its rapid acquisition and cost-effectiveness compared to other medical imaging modalities [3]. However, traditional X-ray systems, while widely used, can delay the life-saving process in time-sensitive situations as it can take up to 8-48 minutes to get a full body scan [4].

Given the critical time delays associated with traditional X-ray systems, the need for a more efficient imaging solution becomes evident. The LODOX[®] Statscan[®] system offers a breakthrough, with its ability to produce full-body scans in under 13 seconds [4], [5], [6]. This represents a significant advancement in trauma care, particularly in scenarios where every second counts, such as mass trauma events [7], [8], [9]. Its reduced radiation dose further mitigates the risks associated with repeated imaging, making it a preferred choice in emergency settings [7].

Despite its advantages, the LODOX[®] Statscan[®] faces the challenge of high noise levels which comprises image quality. De Villiers showed that this increased noise is primarily due to the low X-ray dose used [10]. LODOX[®] has sought to improve this by replacing the [Charge Coupled Detector \(CCD\)](#) with [Photon Counting Detector \(PCD\)](#) [11]. While studies have shown that [PCD](#) technology does not increase noise in [Computed Tomography \(CT\)](#) scans [12], there is concern that its introduction

to LODOX[®] Statscan[®] systems may exacerbate the existing noise issue, potentially affecting diagnostic accuracy. This highlights the critical need for customised denoising algorithms for LODOX[®] Statscan[®], which is the focus of this project.

1.2 Motivation

The increasing noise levels in LODOX[®] Statscan[®] images due to low X-ray dose pose a significant challenge to maintaining diagnostic accuracy [10]. Despite extensive research on denoising in traditional X-rays, CT scans, and ultrasound, the specific challenges posed by noise in LODOX[®] Statscan[®] images remain under-explored, creating a critical gap that this research aims to address. With the growing adoption of LODOX scanners in trauma centres worldwide [6], [13], the unresolved noise issues threaten to undermine the very benefits that make these scanners invaluable in emergency care. By developing an effective denoising model for LODOX[®] Statscan[®] images, this research not only seeks to enhance image clarity but also aims to ensure that the advantages of low-dose imaging do not come at the cost of diagnostic accuracy.

1.3 Problem Statement

The central research question is: "How can noise in Lodox Statscan images be effectively modelled and reduced while preserving their diagnostic quality and accuracy in trauma care?" Given the unique challenges of low-dose imaging and the incorporation of the PCD, this research aims to explore whether specialised denoising algorithms can be developed to overcome these issues. Although techniques like BM3D have proven effective in conventional CT scans [14], they may not be directly applicable to LODOX[®] Statscan[®] images due to the specific noise characteristics introduced by low-dose, highlighting the need for a customised approach.

1.4 Objectives

The main objective of this thesis is to develop a robust denoising model for Lodox Statscan images.

This can further be broken down into the following set objectives:

1. Review and compare existing denoising methods used in medical imaging, specifically X-ray imaging.
2. Adapt or develop new signal processing and/or machine learning techniques for noise reduction in LODOX[®] Statscan[®] images.
3. Validate the proposed model using imaging phantoms and determine optimal parameters for noise reduction.

4. Develop a user interface that goes along with the denoising algorithm to enable easy user access and use.

1.5 Thesis Contributions

The main contributions of this thesis are as follows:

1. A comprehensive review of current denoising techniques for medical imaging.
2. Development of a novel denoising model specifically designed for LODOX[®] Statscan[®] images.
3. Implementation and evaluation of the proposed model, demonstrating its effectiveness in reducing noise while preserving image quality.

1.6 Scope and Limitations

This project solely focuses on enhancing LODOX[®] Statscan[®] image quality by developing a custom denoising model using controlled non-anthropomorphic phantom studies, and it does not extend to clinical trials. The choice of non-anthropomorphic phantoms, including those provided by LODOX[®] and carefully selected everyday objects, is driven by their ability to simulate relevant imaging conditions while staying within project constraints. The exclusive focus on phantom studies limits the ability to translate findings to clinical practice directly, and additional validation in a clinical setting would be necessary to confirm the model's efficacy in real-world trauma scenarios. Additionally, given the model's design specifically for LODOX[®] Statscan[®] images, adaptation to other low-dose imaging systems may require additional tuning to accommodate different noise profiles. While these limitations confine the current study, they also highlight areas for future research, including clinical validation and the exploration of more comprehensive denoising models.

1.7 Thesis Outline

The remainder of this thesis is organized as follows:

Chapter 2, Literature Review: Reviews the theoretical foundations and related work in medical imaging and denoising techniques.

Chapter 3, Methodology: Details the research design, data collection methods, and the development of the denoising model.

Chapter 4, Design: Discusses the implementation of the denoising algorithms and the computational framework

Chapter 5, Results: Presents the findings from evaluating the denoising model.

Chapter 6, Conclusions: Summarizes the research contributions, discusses limitations, and suggests directions for future work.

Chapter 2

Literature Review

This chapter assesses existing medical imaging denoising techniques, specifically focusing on their applicability to LODOX[®] Statscan[®] images. It starts with a review of X-ray imaging theory, establishing a foundation to understand the unique challenges posed by LODOX[®] Statscan[®] system. After that, it delves into a discussion of the specific image artifacts associated with this technology. Finally, denoising algorithms used in Medical imaging are critically evaluated, assessing their suitability to LODOX[®] Statscan[®] images.

2.1 X-ray Imaging Fundamentals

This section summarises the theoretical framework and principles of X-ray imaging. Understanding the core principles of X-ray imaging is fundamental to improving the X-ray imaging quality through denoising, particularly in the context of low-dose systems like LODOX[®] Statscan[®]. The following subsections will look into mechanisms of X-ray production, X-ray detection and image formation.

The fundamental X-ray imaging theory, including X-ray generation, interaction with matter, and image formation, is extensively covered in [15], [16], [17], providing a solid foundation for the subsequent discussion.

2.1.1 X-ray Production

X-rays are generated in an X-ray tube by accelerating high kinetic energy electrons from the cathode across the electrostatic field in the vacuum towards the anode, striking the anode emitting X-rays.

X-ray emission is primarily controlled by the anode voltage, which dictates the maximum energy of the X-ray photons, and the tube current, which determines the photon flux. These parameters directly influence image quality by affecting the photon count detected by the X-ray detectors. Additionally, the focal spot size of the X-ray tube plays a crucial role in image resolution as it determines the size

of the X-ray beam. For instance, when the image details to be captured are smaller than the X-ray beam diameter, geometric blur is observed, which degrades image quality.

X-ray production is only one part of the imaging process; once generated, these Xrays must travel through various tissues, where their attenuation plays a critical role in the resulting image quality.

2.1.2 X-ray Attenuation

X-ray attenuation across various bodies is what brings about X-ray contrast. X-ray attenuation occurs when the X-ray photons collide with other atoms and get deflected from their path whilst losing some energy. The major forms of X-ray attenuation are Rayleigh Scattering, Compton Scattering, Photoelectric effect and pair production. These are summarised in the Table 2.1 below:

Interaction	Photon Energy Range	Significance in Medical Imaging
Rayleigh Scattering	Low Photon Energies	Negligible Above 50 keV thus negligible influence on image quality
Compton Scattering	All Photon Energies	Characteristic radiation leading to scattering that causes haze in the images.
Photoelectric Effect	50-70 keV	Crucial for X-ray contrast, especially at lower energies
Pair Production	Above 1.02 MeV	Limited relevance in medical imaging as rarely seen in practice

Table 2.1: Summary of Photon Interaction Mechanisms and Their Significance in Medical Imaging.

In LODOX® Statscan®, scattering is not an issue due to the unique detector architecture that reduces scattering by up to 95% [5]. As X-rays are attenuated as they pass through different tissues, this varying absorption information must be recorded to generate X-ray images. The following subsection will look into the X-ray detection and image formation mechanism and how it affects the image quality.

2.1.3 X-ray Detection and Image Formation

This subsection delves into how X-ray photons are converted and detected for imaging. X-ray intensity is primarily measured using photographic films and digital detectors, necessitating conversion to another energy form, usually visible light or [Ultraviolet rays \(UV\)](#) photons. Digital detectors are predominantly used today, as older photographic films and fluoroscope detectors were phased out due to their very low quantum efficiency and sensitivity.

During the conversion process, these digital detectors introduce various noise components, including electronic noise and quantum noise due to the use of [application-specific integrated circuits \(ASIC\)](#). In addition, converting X-ray photons into electrical signals can introduce image artifacts such as detector blur. Detector blur occurs due to the conversion layer, which typically emits visible light in all directions. A thick conversion layer increases the likelihood of cross-talk between neighbouring pixels, while a thinner conversion layer reduces this effect and lowers quantum efficiency. Keeping the conversion layer close to the detector element can help mitigate detector blur.

Motion blur is another significant factor impacting image quality, which arises when the patient moves during exposure due to breathing. High detector sensitivity and a high photon flux from the X-ray source can allow for shorter exposure times, which reduces the likelihood of motion blur affecting the final image.

2.2 Noise in X-ray imaging

This section will examine the various types of noise inherent in X-ray imaging, specifically low-dose X-ray imaging systems such as the LODOX[®] Statscan[®]. It then proceeds to discuss the sources of these noises in the LODOX[®] Statscan[®] and concludes with an analysis of the impact of the noise on image quality and diagnosis.

2.2.1 Types of Noise in X-ray Imaging

Noise is defined as random unwanted stochastic fluctuations and variations in brightness and colour information in an image [18], [19]. In X-ray, there are various noise types, each with a different statistical model arising from multiple sources such as the detectors' inherent properties, X-ray source, inspected objects and controller circuits [20], [21]. The primary noise present in X-rays is Quantum noise. Other prominent noise types include Electronic and Anatomical noise. These three noise types are discussed below:

Quantum Noise

Studies show that quantum noise is predominant in [Photon Counting Detector \(PCD\)](#) [21], [22]. Given that [PCD](#) are the detectors currently being used in the LODOX[®] Statscan[®] it is paramount to understand quantum noise. Quantum noise results primarily from X-ray photon detection and conversion [23], [20]. It is produced due to the random accumulation and distribution of the X-ray photons on the detectors' surface [21], [18], [24], [25], [3]. This is shown in the Figure 2.1 below:

Due to the wide spectrum energy of X-ray photons and the randomness mentioned above, quantum noise is modelled using the Poisson distribution as shown below:

$$P(x) = e^{-\lambda t} \frac{(\lambda t)^k}{x!} \quad (2.1)$$

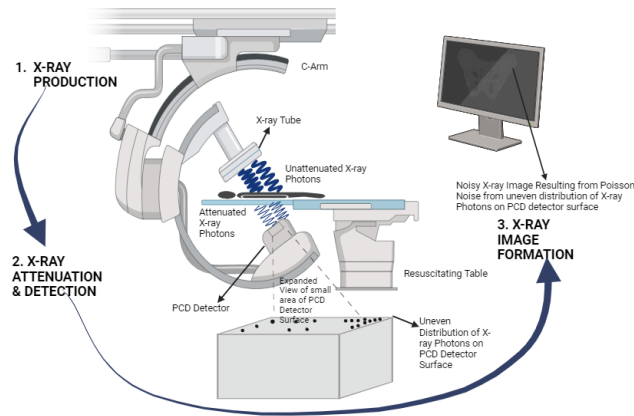


Figure 2.1: Diagram illustrating the generation of quantum noise in X-ray imaging due to the uneven distribution of X-ray photons on the PCD detector surface, resulting in a noisy image output. Created with [BioRender.com](https://www.biorender.com)

Where:

- $P(x)$: probability of distribution of photons
- λ : Expected number of photons
- X : measured number of photons
- t : given time interval

Equation 2.1 depicts the signal-dependent nature of quantum noise, indicating it is not an additive noise like [Additive White Gaussian Noise \(AWGN\)](#) as shown in studies [26], [27], [25]. Since quantum noise follows Poisson distribution, the expected photon count ($E(x)$) is equal to the variance of the photon count ($\text{var}(x)$) over the given time interval in Equation 2.1. Thus quantum noise is proportional to the square root of the number of photons captured by the detector [25] and the square root of radiation exposure [22] as shown in equations 2.2 and 2.3 below:

$$\begin{aligned} E[x] &= \text{var}[x] = \lambda t \\ \text{std}[x] &= \sqrt{\lambda t} \end{aligned} \tag{2.2}$$

$$\sqrt{\text{exposurelevel}} \tag{2.3}$$

From the above, it can be deduced that by increasing the X-ray radiation and exposure time, quantum noise can be reduced [25]; however, this is not a suitable method in the LODOX[®] Statscan[®] system as it is inherently a low-dose X-ray system.

Electronic Noise

Electronic noise typically arises from random signals caused by thermal fluctuations in interconnected electronics [28], amplifier noise [29], and imperfections in detectors, such as thickness variations, scratches, and dust on the detector substrate [20]. Additionally, voltage variations over the long signal

distances in large detectors contribute to this noise [23]. This type of noise is prevalent in [Charge Coupled Detector \(CCD\)](#) [28] and is most pronounced at lower X-ray energy levels [18].

Electronic noise is modelled using the Gaussian distribution as shown in Equation 2.4 as it emanates from random signals [3]:

$$G(x) = \left(\frac{1}{\sigma\sqrt{2\pi}} \right) e^{-\frac{(x-\mu)^2}{2\sigma^2}} \quad (2.4)$$

Where:

- σ : represents the standard deviation
- X : represents the value of the pixel
- μ : represents the mean

Since the LODOX[®] Statscan[®] now uses [PCD](#) instead of [CCD](#), the impact of electronic noise is significantly reduced, with the primary source being the low X-ray doses used.

Anatomical Noise

Anatomical noise is caused by the projection of the 3D object of interest to a 2D plane, resulting in the overlapping of anatomical objects in the region of interest in the image [18], [20]. This overlap leads to local and global camouflaging that obstructs critical parts of the image [20]. Studies have shown that anatomical noise is particularly prevalent at very low X-ray energy levels [18]. Notably, anatomical noise is one of the most challenging to correct and affects all X-ray systems [20].

2.2.2 Impact of Noise on Image Quality and Diagnosis

Noise in X-ray systems significantly impacts image quality, particularly at low doses [18]. It can introduce obstructions that render images non-diagnostic [24]. Additionally, it can introduce artifacts that hinder the acquisition of quality images, potentially leading to false diagnoses [29]. Moreover, degradation in image quality makes visual interpretation difficult [30], [19], complicating diagnostics for medical professionals [26]. Finally, the corruption of X-ray images due to noise further impairs diagnostic accuracy [25], [31], [32] ultimately hindering effective clinical decision-making.

2.3 Denoising

From section 2.2.2, it has been established that noise degrades the image quality, thus making denoising a critical part of the pre-processing chain. The primary objective of denoising is to effectively suppress noise while preserving the image integrity [3], [19], [33]. Broadly, there are three X-ray denoising methods, as shown below:

1. **Use of customised hardware:** Done through incorporating hardware filters such as Aluminium filters in the X-ray machines to help reduce noise [34].

2. **Increase in X-ray dose:** An increase in the X-ray dose used significantly reduces the noise in the image. However, the dose is hindered by the Maximum Permissible Dose(MPD); thus, the dose cannot be arbitrarily increased [35].
3. **Digital Denoising Algorithms:** Involves using digital image processing algorithms to reduce the noise digitally.

Digital denoising algorithms are widely used as they are not as expensive as hardware customisation and do not increase radiation risk to the patients as the increasing X-ray dose method, thus making it the most effective technique to consider for denoising LODOX[®] Statscan[®] images.

The type of noise in the images significantly impacts the effectiveness of denoising algorithms, and studies caution against the assumption that all noise is [AWGN](#) [35]. As highlighted in Section 2.2.1, quantum noise is the most common in X-ray images, especially in low-dose settings. Consequently, noise-independent denoising algorithms do not work well on X-ray images, making Poisson-based methods the preferred approach [27], [36]. Studies have suggested two approaches to handle Poisson noise, as discussed below:

1. **Poisson Direct Denoising methods:** Model the Poisson noise statistics, which are usually helpful when the images suffer from very high noise levels [35], [36].
2. **Poisson [Variance Stabilising Transform \(VST\)](#) Denoising methods:** Involves transforming the Poisson noise to Gaussian noise because when the photon count is large enough, Poisson distribution approaches Gaussian, and the [Anscombe transform](#) is used to stabilising the variance of the Poisson noise [36].

However, denoising X-ray images presents several critical challenges discussed below:

1. **Maintaining flat regions:** Flat regions in the image must remain flat without introducing noise or artifacts [3].
2. **Preserving image boundaries:** Image boundaries must be retained without causing blurring [3].
3. **Protecting global contrast and textural features:** The global contrast should be preserved, and textural details should not be lost [19].
4. **Avoiding new artifacts:** The denoising process should not generate any new artifacts in the image [3], [27].

Over the years, various algorithms have been proposed to address these four challenges. These algorithms are generally classified into three broad categories: Classical Filters, Hybrid Filters and Deep learning methods [3], [35]. The following section will analyse each category in detail, exploring their advantages, disadvantages, and suitability for handling Poisson noise in the LODOX[®] Statscan[®].

2.3.1 Classical Filters

This subsection briefly discusses the classical [Digital Signal Processing \(DSP\)](#) filters implemented to combat noise in X-ray Images, broadly classified into spatial and transform filters. Spatial filters are further categorised into linear and non-linear filters. Linear filters are easy to implement as they apply non-discriminate denoising to all the pixels without prior categorisation [26] and thus are not good with signal-dependent noise leading to artifacts and blurring [3], [37]. In contrast, non-linear filters first detect noisy pixels and then replace them selectively, making them more effective for denoising [26].

Spatial Domain Filters

This subsection discusses key spatial domain filters currently used for X-ray image denoising. A detailed analysis of these filters, outlining their strengths, weaknesses, and applicability to LODOX[®] Statscan[®] images, is discussed below.

[Anisotropic Diffusion Filter \(ADF\)](#) is a spatial diffusion filter that adaptively smooths images, preserving important anatomical structures by controlling diffusion across edges [25]. Although [ADF](#) effectively preserves micro-texture and edges, its performance degrades with larger mask sizes, reducing its ability to handle quantum noise [25]. Additionally, [ADF](#) is slow, and its effectiveness depends heavily on careful parameter selection, and when not done correctly it tends to remove some image details degrading image quality [3], [25]. Consequently, this makes [ADF](#) less suitable for the high levels of quantum noise in LODOX[®] Statscan[®] images.

Despite [ADF](#)'s ability to maintain micro-texture and edges, its shortcomings in dealing with quantum noise in LODOX[®] Statscan[®] images make exploring alternative techniques, such as the [Bilateral Filter \(BF\)](#), necessary. [BF](#) is a non-iterative filter that merges grey levels of pixels based on their spatial and photometric similarity, preserving sharp structural patterns while suppressing noise [3], [25]. However, [BF](#) is prone to gradient reversal artifacts near edges, leading to a loss of fine detail [3], [25]. Kirti et al. [27], [38] attempted to address this by developing an enhanced version, [Poisson Reducing Bilateral Filter \(PRBF\)](#), adding the capability to remove Poisson Noise, although it still struggles with photon-limited images. Given that LODOX[®] Statscan[®] images are photon-limited, the [BF](#) may not be ideal for denoising.

Since [BF](#) struggles with photon-limited images, exploring other filters that can effectively handle quantum noise, such as [Total Variation \(TV\)](#) filters, is necessary. [TV](#) filter popularly known as [Rudin-Osher-Fatemi model \(ROF\)](#) was first developed by Rudin et al. [39] and is an edge-preserving algorithm designed to handle discontinuities in anatomical details [26], [40]. Studies show that [TV](#) is effective in denoising Poisson and Gaussian noise [40]; however, it struggles to preserve edges, produces the [Staircase effect](#) [40] and has long processing times [41]. Over time researchers have sought to address these challenges by improving the initial version of the [TV](#) algorithm. Some of these adaptations are summarised in Table 2.2 below:

Algorithm	Description	Challenges
Richardson-Lucy algorithm (R-L) and TV (Dey et al.) [42]	Combined R-L and TV to develop a Poisson-based denoising algorithm specifically suited for microscopy images.	Only Tailored for microscopy images
Modified Rudin-Osher-Fatemi model (MROF) (Triet et al.) [43]	An improved version of ROF that can process Poisson noise.	Long execution times, Artificial artifacts, Cannot handle photon-limited images.
Adaptive Total Variation method (ATV) (Prasath) [44]	Developed to address artificial artifacts in MROF.	Faces the same challenges as MROF.
Enhanced ATV (Liu et al.) [45]	Modified ATV to denoise photon-limited images.	Long execution times.

Table 2.2: Summary of Adaptations to TV Filters to addressing challenges in original TV filter.

Non-Local Means (NLM) has emerged as an alternative to denoise photon-limited images to address the shortcomings of TV filters. NLM uses a non-local averaging technique that operates on all similar pixels, removing noise after exploring redundant information [3], [26], [40]. Consequently, this leads to high detail preservation in images [40]. However, despite the high detail preservation, NLM suffers from slow execution time due to the computational overhead arising from the complexity of evaluating the pixel weights [3], [40]. Various researchers have proposed solutions to address the challenges, as summarised in Table 2.3 below:

Researcher(s)	Proposed Solution	Challenges Addressed
Mahmoudi and Sapiro [46]	Modified NLM by adding Pre-selection of neighborhoods	Increased speed
Pierrick Coupe [47]	Added parallel processing	Improved execution time
Deledalle et al. [48]	Modified NLM to incorporate Poisson noise statistics	Tailored for Poisson noise
Shim et al. [49]	Implemented Fast Non-Local Means (FNLM)	Significant speed improvement i.e 3.7 times faster than TV filter

Lee et al. [34]	Combined NLM denoising algorithm with Aluminium additive hardware filters	Superior results in Contrast to Noise Ratio (CNR), Coefficient of Variation (COV), Natural Image Quality Evaluator (NIQE), and Blind/Referenceless Image Spatial Quality Evaluator (BRISQUE)
Lee [41]	FNLM with acceleration function and Euclidean distance	Superior Normalized Noise Power Spectrum (NNPS), CNR, and COV values; fast processing time (0.17s)

Table 2.3: Summary of Proposed Solutions to Address Challenges in NLM Filter

NLM filters still suffer from slow execution due to computational complexity and require high-speed hardware to execute faster, thus limiting their suitability for denoising LODOX[®] Statscan[®] images.

Transform Domain Filters

This subsection details some transform domain filters used in X-ray image denoising. Unlike spatial filters, transform domain filters operate by converting the image into an alternative representation, such as the Wavelet or Fourier domain, where denoising is performed, after which the image is transformed back to the spatial domain using an inverse transform. A detailed analysis of these filters, outlining their strengths, weaknesses, and applicability to LODOX[®] Statscan[®] images, is discussed below.

Gaussian filter is the most widely used transform domain filter known for reducing edge blurring and computational efficiency; however, it loses a lot of image detail [3] , [26]. Given that Gaussian filter works is tailored for Gaussian noise, it struggles to denoise Poisson noise prevalent in LODOX[®] Statscan[®]. Researchers have opted for other transform domain filters to denoise X-ray images to address these shortcomings.

One of the filters that has shown promise in improving the shortcomings of the Gaussian filter is the wiener filter. It is an Mean Squared Error (MSE)-optimal stationary filter that balances noise smoothing and inverse filtering, using local image variance for adaptive smoothing [3], [25], [50]. Studies have shown that the wiener filter effectively reduces Gaussian impulse and speckle noise whilst preserving the edges [25], [51]. However, despite these advantages, it only provides a point estimate that gives optimal results under specific conditions, making it less effective in handling signal-dependent noises such as Poisson [3]. Additionally, it leads to blurry images due to the use of fixed kernel size [25].

Researchers have attempted to improve the Wiener filter to enhance its performance. For instance,

Goreke [52] modified a wiener filter by incorporating an [finite impulse response \(FIR\)](#) filter with [Atom Search Optimization \(ASO\)](#) optimisation, demonstrating its superiority over [NLM](#), [BF](#), [Block Matching](#) and [3D filtering \(BM3D\)](#), [Poisson Unbiased Risk Estimation – Linear Expansion of Thresholds \(PURE-LET\)](#), [Bayes](#), and [dual tree complex wavelet transform \(DTCWT\)](#) filters in terms of contrast index, entropy, sharpness, and computational efficiency. Additionally, Lahmiri [19] developed a multistep iterative Wiener filter where the denoised output from one step is the input to the next stage, stopping based on an energy condition and showed that it could denoise and restore the original texture in finite iterations. However, this approach was limited to Gaussian noise [19], reducing its applicability to other noise types. Despite these improvements, the Wiener filter still struggles to handle Poisson noise, making it a less suitable option for [LODOX[®]](#) [Statscan[®]](#) images, which are predominantly degraded by Poisson noise.

While the wiener filter preserves the image texture, its limitations in handling quantum noise suggest that complementary methods, such as wavelet filters, are necessary for optimal denoising. Primarily, wavelet filters operate by applying shrinkage or thresholding to wavelet coefficients, followed by image synthesis [40]. The local definition of features allows wavelet filters to preserve minute edges and details in X-ray images [3], [40]. Notably, wavelet filters are associated with challenges of estimating an appropriate threshold and the tendency to introduce artifacts leading to smooth edges at times [3], [40]. To address these challenges associated with the wavelet filter, researchers have developed various variations, which are summarised in Table 2.4 below:

Researcher(s)	Method & Description	Strengths	Limitations
Thierry et al. [53]	PURE-LET : Based on the un-normalised Haar wavelet transform, the minimisation of unbiased MSE estimate	Handles Poisson noise. Competitive in denoising and computational complexity	Cannot handle photon-limited images
Timmermann and Nowak [54]	Multiscale Multiplicative Innovations (MMI) Model: A simple Bayesian intensity estimate procedure	Denoises photon-limited images	Highly complex
Zhang et al. [55]	multiscale variance stabilizing transform (MS-VST) : Extension of Anscombe transform combining wavelet, ridgelet, and curvelet	Denoises photon-limited images	Highly complex

Wang [51]	Adaptive Wavelet Wiener Filter: Pre-processing, three-wavelet decomposition using Daubechies wavelet (db5), improved threshold shrinkage (IBS)	Superior performance in preserving edges, enhancing image quality in low-dose X-ray and medical images	Highly complex
Kaur et al. [56]	Wavelet-Based Statistical: Uses realistic distribution of wavelet coefficients	Better feature preservation in medical images	Highly complex
Du et al. [57]	DTCWT : Dual-tree complex wavelet transform	Better than wavelet transform filters in Poisson noise reduction in X-ray images	Highly complex

Table 2.4: Summary of Wavelet Filter Variations for Poisson Noise Reduction in Medical and X-ray Images, Highlighting Strengths and Challenges

The wavelet filter has proven effective in denoising photon-limited images by preserving fine edges and details while reducing Poisson noise. Despite challenges such as determining the optimal threshold and potential edge smoothing, advanced variations like [IBS](#) techniques have enhanced its performance. These methods, particularly when using Daubechies wavelet (db5), demonstrate superior capability in handling low-dose X-ray images, making wavelet filters a potential denoiser for LODOX[®] Statscan[®] images.

2.3.2 Hybrid Filters

Hybrid filters have gained popularity for X-ray image denoising due to the non-adaptability of classical filters, as they are suited to handling specific types of noises. Hybrid filters include filters that combine two or more classical filters or use entirely non-classical spatial and transform methods to denoise the images. This subsection summarises the most notable hybrid filter approaches, strengths, and limitations.

One of the most successful hybrid filters is 3D transform domain filtering. These methods convert 2D images into 3D domain and apply a sliding window to process the blocks, matching similar regions to effectively reduce noise through shrinking coefficients in the 3D arrays [40]. The most widely used 3D domain filter is the [BM3D](#), which is known for its significant noise reduction while preserving local texture information [25]. However, [BM3D](#) faces challenges when the image is heavily contaminated with noise, leading to overshooting, which can obscure the structural information in X-ray images [25].

Over time, researchers have developed various [BM3D](#) modifications to address the abovementioned challenges. For instance, Makitalo et al. [58] modified the [BM3D](#) for Poisson noise by incorporating an [Anscombe transform](#) to stabilise the variance of Poisson-corrupted images. Additionally, Harrison et al. [14] developed a custom version of [BM3D](#) specifically for [Photon-counting CT \(PCCT\)](#) scanners called [BM3D_PCCT](#) that uses four energy thresholds and exploits correlation and exact alignment between energy bins to denoise the images. They demonstrated that [BM3D_PCCT](#) achieved a 65.0% reduction in noise standard deviation, tighter clustering of attenuation values, and smaller mean angular differences compared to [BM3D](#) [14]. Ren [59] also developed a denoising method based on subspace decomposition, employing sparse representation and block matching to suppress noise. In simulations using a three-dimensional digital mouse phantom, Ren's method improved the peak signal-to-noise ratio by 2.21 dB compared to existing techniques when the photon flux was 4×10^3 [59].

Although [BM3D](#) is the most widely used hybrid filter, several other filters have been developed to address its shortcomings. However, most of these alternatives are not widely adopted. Table 2.5 below summarises these filters.

Researcher	Hybrid Method	Filter	Advantages	Limitations
Salmon et al. [60]	Non-local	Principal Component Analysis (PCA)	Better noise reduction compared to BM3D	Increased execution time due to iterative nature; struggles with noise detection in high-dimensional data.
Kipele [36]	PCA combined with NLM		Performs well in reducing noise in images with moderate intensity	Performance not tested for extreme Poisson noise levels.
Wensen et al. [61]	Hybrid Poisson (HNIPM) trained on Anscombe transform	Non-iterative Model	Removes Poisson noise in both high and low-peak images	Long execution time; not suitable for photon-limited images.
Jisha & Suresh [62]	Anscombe transform with Curvelet and MS-VST		Performs better than most wavelet-based filters	Execution time may be high; tested on specific noise types.

Dong [32]	Wavelet filter combined with median filter	Preserves image details while reducing noise	Tested only on Gaussian and Salt-and-Pepper noise; efficacy on Poisson noise not verified.
Dabov et al. [63]	Non-local adaptive nonparametric filtering	Similar performance to NLM and Yaroslavsky filter	Limited testing on medical X-ray images; complex computational process.
He et al. [64]	Guided filter	Superior performance compared to bilateral filter; reduces quantum noise	Dependent on parameter selection and guidance image; large filter masks lead to blurring.
Treece et al. [65]	Bitonic filter	Effectively reduces noise without artifacts; good edge preservation	Can cause significant blurring if not carefully applied.
Mandic et al. [37]	Local Polynomial Approximation - Relative Intersection of Confidence Intervals (LPA-RICI) adaptive algorithm	Less execution time due to easy parallelisation	Limited testing on specific noise types.
Umadevi et al. [31]	Bi-orthogonal Haar wavelets with BayesShrink thresholding and Independent Component Analysis (ICA)	Achieves high-quality images quickly (PSNR = 44.85)	May not work as efficiently in photon-limited settings.
Kirti [35]	Hybrid filter combining non-local means and BM3D collaborative filtering	Encouraging results with Poisson noise; improved PSNR over wavelet-based methods	Execution time still an issue compared to faster filters.

Table 2.5: Summary of Hybrid Filters for X-ray Image Denoising

Hybrid filters have emerged as an effective solution for addressing the limitations of classical filters by

combining multiple techniques to handle different types of noise. These filters, such as those based on [PCA](#), curvelet transforms, and adaptive models, show improved noise reduction, edge preservation, and execution efficiency. Notably, hybrid methods like adaptive wavelet Wiener preprocessing and variations of [BM3D](#) tailored for Poisson noise have demonstrated superior performance in enhancing image quality in medical X-ray imaging, making them well-suited for the complex noise characteristics present in LODOX[®] Statscan[®] images.

2.3.3 Deep Learning Methods

This subsection provides a brief overview of [Machine Learning \(ML\)](#) methods applied to medical imaging denoising, highlighting their advantages and associated challenges.

Machine learning, particularly deep learning, has transformed data processing by solving complex problems, including medical image denoising. Deep learning employs artificial neural networks to learn the characteristics of a given problem and develop effective solutions. In medical image denoising, ML models are trained to identify and remove noise patterns from the images. These models fall into two broad categories: supervised learning, which requires clean, labelled data (ground truth), and unsupervised learning, which does not require ground truth data. Unsupervised learning models are preferred as in clinical settings, acquiring noise-free data in medical imaging is impractical, except through simulations, which may not always accurately reflect real-world conditions [66].

The shift from conventional filters to [ML](#) methods has been driven by several challenges. Studies have shown that the manual selection of filters is a cumbersome process requiring good domain knowledge [3]. Additionally, many conventional filters rely on prior noise information, further complicating optimisation [3]. In contrast, ML methods require relatively few tuning parameters and learn by themselves to denoise images [67]. For instance, [Convolutional Neural Networks \(CNN\)](#) excel at extracting relevant features from noisy data and can be trained efficiently using parallel processing with [Graphical Processing Unit \(GPU\)](#)s [3]. This makes [ML](#) methods more efficient than conventional filters in many cases.

The following will explore several specific applications of deep learning frameworks that denoise X-ray images with a specific focus on unsupervised models. [Noise2Noise \(N2N\)](#) and [Noise2Void \(N2V\)](#) are the two most common unsupervised deep learning denoising methods that have been used in medical image denoising as they do not require clean reference images, making them well-suited for applications such as LODOX[®] Statscan[®] image denoising.

Lehtinen et al. [68] developed [N2N](#) to address the challenge of requiring clean and noisy image pairs during the model training phase. [N2N](#) makes use of two noisy images each with an independent noise distribution to learn the underlying signal from these noise-corrupted data points. Studies have shown [N2N](#) achieving comparable performance to models trained with clean images. For instance,

Lehtinen et al. [68] trained the N2N for 300 epochs with noisy targets and achieved an average Peak Signal-to-Noise Ratio (PSNR) of 31.10 dB on the validation set, while training with clean targets reached 31.14 dB, comparable to previous work by Wang et al. [69] and Lee et al. [70]. Additionally, N2N can generalise across various types of noise distributions [68]. The use of noisy image pairs during training and adapting to various noise types makes N2N a highly suitable model for denoising LODOX[®] Statscan[®] images where noise is prevalent and acquiring images is impossible.

Krull et al. [71] developed N2V to eliminate the need for paired noisy images during the training phase. N2V uses single noisy images to train the network to predict the values of randomly masked pixels, encouraging the model to learn spatial relationships in the data. This makes N2V highly adaptable to various noise types as minimal assumptions about the underlying noise distribution are made. Krull et al. [71] demonstrated N2V applicability to various imaging modalities by running experiments on photography, fluorescence microscopy, and cryo-Transmission Electron Microscopy. They concluded that as long as the assumptions of predictable signal and pixel-wise independent noise are met, N2V performance is comparable to traditional and N2N-trained models [71]. Since N2V does not require clean images or paired noisy images, it is a highly scalable solution, well-suited for LODOX[®] Statscan[®] images.

Both Noise2Noise and Noise2Void are promising models for medical image denoising due to their unsupervised nature, effectively addressing the challenges of acquiring clean training data in a clinical context like Lodox imaging.

Other attempts to denoise X-ray images primarily using supervised learning are summarised in Table 2.6 below:

Author(s)	Proposed Model	Strengths	Challenges
Zhang et al. [72]	denoising convolutional neural networks (DnCNN): Neural network that outputs residual noise (V) and computes clean X-ray (C) as the sum of noisy observation and residual image	Outperforms BM3D and Weighted nuclear norm minimization (WNNM)	Not effective for Poisson noise
Hariharan [66]	Learning-based model using model-based simulations and data-driven normalisation for robust denoising	Outperforms BM3D and WNNM; produces visually superior results	Limited clinical practicality due to reliance on simulated data

Nadkarni et al. [67]	Custom 2-D U-Net CNN for quick iterative reconstruction and accurate material decomposition across energy thresholds	15 times faster than iterative reconstruction; higher spatial resolution	Relies on supervised learning and high computational resources; training detector prone to distortions
Huber et al. [12]	CNN model using U-Net for ultra-high-resolution PCD Computed Tomography (CT), trained with image-based noise insertion	Retains fine details and low contrast signals; preferred by radiologists	Limited by supervised learning and high-quality training data requirements
Chang et al. [73]	prior knowledge-aware iterative denoising neural network (PKAID-Net) using prior knowledge-aware iterative denoising neural network using lower-noise Virtual Monoenergetic Images (VMI) for improved denoising	96% noise reduction; maintains spatial and spectral fidelity	Potentially complex iterative refinement may limit practical application
Baffour et al. [74]	CNN model for detecting multiple myeloma using PCD CT images	Enhanced detection of abnormalities; better clarity and accuracy	Focused on detection and denoising only a small subset
Durcos et al. [75]	Uses regularisation strategy to suppress noise	Easy to implement	Limited noise suppression effect across various noise types
Zhang et al. [76]	Third-Order Tensor Model that combines TV regularisation with tensor similarity and image sparsity	Improved noise suppression	High computational costs due to tensor reconstruction

Sun et al. [77]	FBPTransNet	that	Outperforms TV	and	Does not clearly address Poisson
	combines U-Net CNN	FBPconvNet;	clearer	noise	
	with Transformer	image details			
	module for improved				
	image detail restora-				
	tion				

Table 2.6: Summary of Deep Learning Approaches for X-Ray Image Denoising

2.4 Conclusion

The literature review provided a comprehensive analysis of classical and modern denoising techniques, mainly focusing on their applicability to low-dose systems such as the LODOX[®] Statscan[®] systems.

The review began with a brief overview of X-ray imaging fundamentals, including X-ray production, attenuation, and detection and their significance to image quality. This was followed by an analysis of noise types in X-ray images. It was highlighted that the predominant noise degrading X-ray images is Poisson noise, and various Poisson denoising methods were looked into. A plethora of classical DSP filters was looked into, highlighting their limitations in handling photon-limited images. Despite some variations of wavelet and NLM filters showing promise, they often fell short of effectively reducing Poisson noise without compromising image quality. The review then transitions to hybrid filters, particularly the BM3D. BM3D demonstrates significant improvement over classical filters but still faces challenges in denoising noise-heavy images such as LODOX[®] Statscan[®] images. This underscored the need for adaptable denoising methods to learn different noise patterns.

ML methods like N2N and N2V offer significant potential due to their ability to operate without clean training data. This is critical for LODOX[®] Statscan[®] as it is impossible to obtain ground truth data. However, in most of the literature, the testing was mostly done on Magnetic Resonance Imaging (MRI), CT and microscopy images, with limited application to low-dose X-ray systems like the LODOX[®] Statscan[®]. While N2N and N2V have shown adaptability across various noise types in other imaging domains, applying these models to the LODOX[®] Statscan[®] system presents both a challenge and an opportunity for further research. This project aims to bridge this gap by adapting and enhancing N2N and N2V models specifically for LODOX[®] Statscan[®] images, documenting the results and challenges encountered in this process. This approach addresses the current limitations in the literature and contributes to the development of more effective denoising techniques for low-dose X-ray imaging.

Chapter 3

Methodology

Chapter 4

Design

Chapter 5

Results

Chapter 6

Conclusions

Bibliography

- [1] C.-Y. Fu, S.-C. Wu, and R.-J. Chen, “Lodox/Statscan provides rapid identification of bullets in multiple gunshot wounds,” *The American Journal of Emergency Medicine*, vol. 26, no. 8, pp. 965.e5–965.e7, Oct. 2008. [Online]. Available: <https://www.sciencedirect.com/science/article/pii/S0735675708001265>
- [2] C.-Y. Fu, Y.-C. Wang, C.-H. Hsieh, and R.-J. Chen, “Lodox/Statscan provides benefits in evaluation of gunshot injuries,” *The American Journal of Emergency Medicine*, vol. 29, no. 7, pp. 823–827, Sep. 2011. [Online]. Available: <https://www.sciencedirect.com/science/article/pii/S0735675711001331>
- [3] M. Juneja, J. S. Minhas, N. Singla, R. Kaur, and P. Jindal, “Denoising techniques for cephalometric x-ray images: A comprehensive review,” *Multimedia Tools and Applications*, vol. 83, no. 17, pp. 49 953–49 991, May 2024. [Online]. Available: <https://doi.org/10.1007/s11042-023-17495-z>
- [4] S. Beningfield, H. Potgieter, A. Nicol, S. van As, G. Bowie, E. Hering, and E. Lätti, “Report on a new type of trauma full-body digital X-ray machine,” *Emergency Radiology*, vol. 10, no. 1, pp. 23–29, Apr. 2003. [Online]. Available: <https://doi.org/10.1007/s10140-003-0271-x>
- [5] B. Amirlak, B. Zakhary, K. Weichman, H. Ahluwalia, A. R. Forse, and R. D. Gaines, “Novel use of Lodox® Statscan® in a level one trauma center,” *Ulus Travma Acil Cerrahi Derg*, vol. 15, no. 6, 2009.
- [6] “Full-body radiography (LODOX Statscan) in trauma and emergency medicine: a report from the first European installation site.” [Online]. Available: <https://journals.sagepub.com/doi/epdf/10.1177/1460408610382493>
- [7] A. K. Exadaktylos, L. M. Benneker, V. Jeger, L. Martinolli, H. M. Bonel, S. Eggli, H. Potgieter, and H. Zimmermann, “Total-body digital X-ray in trauma: An experience report on the first operational full body scanner in Europe and its possible role in ATLS,” *Injury*, vol. 39, no. 5, pp. 525–529, May 2008. [Online]. Available: <https://www.sciencedirect.com/science/article/pii/S0020138307004275>

- [8] Lodox Systems, “Lodox solution for trauma units,” August 2018, accessed: August 8, 2024. [Online Video]. Available: <https://www.youtube.com/watch?v=M6gmVEs5wMs>.
- [9] S. P. Whiley, H. Alves, and S. Grace, “Full-Body X-Ray Imaging to Facilitate Triage: A Potential Aid in High-Volume Emergency Departments,” *Emergency Medicine International*, vol. 2013, no. 1, p. 437078, 2013, _eprint: <https://onlinelibrary.wiley.com/doi/pdf/10.1155/2013/437078>. [Online]. Available: <https://onlinelibrary.wiley.com/doi/abs/10.1155/2013/437078>
- [10] M. D. Villiers, “Limited angle tomography,” Ph.D. dissertation, Dept. Elect. Eng., Univ. of Cape Town, Cape Town, South Africa, June 2004, [Online]. Available: <http://www.dip.ee.uct.ac.za/publications/theses/PhDMattieu.pdf>.
- [11] D. Y. Martin, “Project brief,” <https://amathuba.uct.ac.za>, (Accessed on 10/20/2024).
- [12] N. R. Huber, A. Ferrero, K. Rajendran, F. Baffour, K. N. Glazebrook, F. E. Diehn, A. Inoue, J. G. Fletcher, L. Yu, S. Leng, and C. H. McCollough, “Dedicated convolutional neural network for noise reduction in ultra-high-resolution photon-counting detector computed tomography,” *Physics in Medicine & Biology*, vol. 67, no. 17, p. 175014, Sep. 2022, publisher: IOP Publishing. [Online]. Available: <https://dx.doi.org/10.1088/1361-6560/ac8866>
- [13] D. S. Evangelopoulos, S. Deyle, H. Zimmermann, and A. K. Exadaktylos, “Personal experience with whole-body, low-dosage, digital X-ray scanning (LODOX-Statscan) in trauma,” *Scandinavian Journal of Trauma, Resuscitation and Emergency Medicine*, vol. 17, no. 1, p. 41, Sep. 2009. [Online]. Available: <https://doi.org/10.1186/1757-7241-17-41>
- [14] A. P. Harrison, Z. Xu, A. Pourmorteza, D. A. Bluemke, and D. J. Mollura, “A multichannel block-matching denoising algorithm for spectral photon-counting CT images,” *Medical Physics*, vol. 44, no. 6, pp. 2447–2452, 2017, _eprint: <https://onlinelibrary.wiley.com/doi/pdf/10.1002/mp.12225>. [Online]. Available: <https://onlinelibrary.wiley.com/doi/abs/10.1002/mp.12225>
- [15] M. A. Haidekker, “Introduction,” in *Medical Imaging Technology*, M. A. Haidekker, Ed. New York, NY: Springer, 2013, pp. 1–12. [Online]. Available: https://doi.org/10.1007/978-1-4614-7073-1_1
- [16] —, “X-Ray Projection Imaging,” in *Medical Imaging Technology*, M. A. Haidekker, Ed. New York, NY: Springer, 2013, pp. 13–35. [Online]. Available: https://doi.org/10.1007/978-1-4614-7073-1_2
- [17] —, “Trends in Medical Imaging Technology,” in *Medical Imaging Technology*, M. A. Haidekker, Ed. New York, NY: Springer, 2013, pp. 111–119. [Online]. Available: https://doi.org/10.1007/978-1-4614-7073-1_7

- [18] W. J. H. Veldkamp, L. J. M. Kroft, and J. Geleijns, "Dose and perceived image quality in chest radiography," *European Journal of Radiology*, vol. 72, no. 2, pp. 209–217, Nov. 2009. [Online]. Available: <https://www.sciencedirect.com/science/article/pii/S0720048X09003349>
- [19] S. Lahmiri, "An iterative denoising system based on Wiener filtering with application to biomedical images," *Optics & Laser Technology*, vol. 90, pp. 128–132, May 2017. [Online]. Available: <https://www.sciencedirect.com/science/article/pii/S0030399216304480>
- [20] J. A. Seibert, "Tradeoffs between image quality and dose," *Pediatric Radiology*, vol. 34, no. 3, pp. S183–S195, Oct. 2004. [Online]. Available: <https://doi.org/10.1007/s00247-004-1268-7>
- [21] "Noise Characteristic and its Removal in digital Radiographic System." [Online]. Available: <https://www.ndt.net/article/wcndt00/papers/idn375/idn375.htm>
- [22] W. Huda and R. B. Abrahams, "Radiographic Techniques, Contrast, and Noise in X-Ray Imaging," *American Journal of Roentgenology*, vol. 204, no. 2, pp. W126–W131, Feb. 2015, publisher: American Roentgen Ray Society. [Online]. Available: <https://ajronline.org/doi/full/10.2214/AJR.14.13116>
- [23] D. S. Kim, "Measurements of the noise power spectrum for digital x-ray imaging devices," *Physics in Medicine & Biology*, vol. 69, no. 3, p. 03TR01, Jan. 2024, publisher: IOP Publishing. [Online]. Available: <https://dx.doi.org/10.1088/1361-6560/ad1999>
- [24] E. N. Manson, V. A. Ampoh, E. Fiagbedzi, J. H. Amuasi, J. J. Flether, and C. Schandorf, "Image Noise in Radiography and Tomography: Causes, Effects and Reduction Techniques," *Current Trends in Clinical & Medical Imaging*, vol. 3, no. 4, pp. 86–91, Oct. 2019, publisher: Juniper Publishers. [Online]. Available: <http://juniperpublishers.com/ctcmi/CTCMI.MS.ID.555620.php>
- [25] T. B. Chandra and K. Verma, "Analysis of quantum noise-reducing filters on chest X-ray images: A review," *Measurement*, vol. 153, p. 107426, Mar. 2020. [Online]. Available: <https://www.sciencedirect.com/science/article/pii/S026322411931293X>
- [26] K. B. Khan, A. A. Khaliq, M. Shahid, and J. A. Shah, "A new approach of weighted gradient filter for denoising of medical images in the presence of Poisson noise," *Tehnički vjesnik*, vol. 23, no. 6, pp. 1755–1762, Nov. 2016, publisher: Sveučilište u Slavanskom Brodu, Stojarski fakultet. [Online]. Available: <https://hrcak.srce.hr/clanak/249928>
- [27] D. Thanh, P. Surya, and L. M. Hieu, "A Review on CT and X-Ray Images Denoising Methods," *Informatica*, vol. 43, no. 2, Jun. 2019, number: 2. [Online]. Available: <https://www.informatica.si/index.php/informatica/article/view/2179>
- [28] P. Gravel, G. Beaudoin, and J. De Guise, "A method for modeling noise in medical images," *IEEE Transactions on Medical Imaging*, vol. 23, no. 10, pp. 1221–1232, Oct.

- 2004, conference Name: IEEE Transactions on Medical Imaging. [Online]. Available: <https://ieeexplore.ieee.org/abstract/document/1339429>
- [29] B. Goyal, A. Dogra, S. Agrawal, and B. S. Sohi, “Noise Issues Prevailing in Various Types of Medical Images,” *Biomedical and Pharmacology Journal*, vol. 11, no. 3, pp. 1227–1237, Sep. 2018. [Online]. Available: <https://biomedpharmajournal.org/vol11no3/noise-issues-prevailing-in-various-types-of-medical-images/>
- [30] M. Warner, “Understanding and Managing Noise Sources in X-ray Imaging,” Apr. 2020. [Online]. Available: <https://www.carestream.com/blog/2020/04/21/understanding-and-managing-noise-sources-in-x-ray-imaging/>
- [31] N. Umadevi and D. S. N. Geethalakshmi, “IMPROVED HYBRID MODEL FOR DENOISING POISSON CORRUPTED X-RAY IMAGES,” vol. 3, no. 7, 2011.
- [32] H. Dong, L. Zhao, Y. Shu, and N. N. Xiong, “X-ray image denoising based on wavelet transform and median filter,” *Applied Mathematics and Nonlinear Sciences*, vol. 5, no. 2, pp. 435–442, Jul. 2020. [Online]. Available: <https://sciencedirect.com/article/10.2478/amns.2020.2.00062>
- [33] N. Kumar and M. Nachamai, “Noise Removal and Filtering Techniques used in Medical Images,” *Oriental journal of computer science and technology*, vol. 10, no. 1, pp. 103–113, Mar. 2017. [Online]. Available: <http://www.computerscijournal.org/vol10no1/noise-removal-and-filtering-techniques-used-in-medical-images/>
- [34] S. Lee and Y. Lee, “The impact of improved non-local means denoising algorithm on photon-counting X-ray images using various AI additive filtrations,” *Nuclear Instruments and Methods in Physics Research Section A: Accelerators, Spectrometers, Detectors and Associated Equipment*, vol. 1027, p. 166244, Mar. 2022. [Online]. Available: <https://www.sciencedirect.com/science/article/pii/S0168900221010846>
- [35] T. Kirti, K. Jitendra, and S. Ashok, “Poisson noise reduction from X-ray images by region classification and response median filtering,” *Sādhana*, vol. 42, no. 6, pp. 855–863, Jun. 2017. [Online]. Available: <https://doi.org/10.1007/s12046-017-0654-4>
- [36] D. Kipele and K. Greyson, “Poisson Noise Reduction with Nonlocal-PCA Hybrid Model in Medical X-ray Images,” *Journal of Image and Graphics*, pp. 178–184, Jun. 2023.
- [37] I. Mandić, H. Peić, J. Lerga, and I. Štajduhar, “Denoising of X-ray Images Using the Adaptive Algorithm Based on the LPA-RICI Algorithm,” *Journal of Imaging*, vol. 4, no. 2, p. 34, Feb. 2018, number: 2 Publisher: Multidisciplinary Digital Publishing Institute. [Online]. Available: <https://www.mdpi.com/2313-433X/4/2/34>

- [38] K. V. Thakur, O. H. Damodare, and A. M. Sapkal, "Poisson Noise Reducing Bilateral Filter," *Procedia Computer Science*, vol. 79, pp. 861–865, Jan. 2016. [Online]. Available: <https://www.sciencedirect.com/science/article/pii/S1877050916002180>
- [39] L. I. Rudin, S. Osher, and E. Fatemi, "Nonlinear total variation based noise removal algorithms," *Physica D: Nonlinear Phenomena*, vol. 60, no. 1, pp. 259–268, Nov. 1992. [Online]. Available: <https://www.sciencedirect.com/science/article/pii/016727899290242F>
- [40] I. Rodrigues, J. Sanches, and J. Bioucas-Dias, "Denoising of medical images corrupted by Poisson noise," in *2008 15th IEEE International Conference on Image Processing*, Oct. 2008, pp. 1756–1759, ISSN: 2381-8549. [Online]. Available: <https://ieeexplore.ieee.org/abstract/document/4712115>
- [41] Y. Lee, "X-ray image denoising with fast non-local means (FNLN) approach using acceleration function in CdTe semiconductor photon counting detector (PCD): Monte Carlo simulation study," *Optik*, vol. 172, pp. 456–461, Nov. 2018. [Online]. Available: <https://www.sciencedirect.com/science/article/pii/S0030402618310234>
- [42] N. Dey, L. Blanc-Feraud, C. Zimmer, Z. Kam, J.-C. Olivo-Marin, and J. Zerubia, "A deconvolution method for confocal microscopy with total variation regularization," in *2004 2nd IEEE International Symposium on Biomedical Imaging: Nano to Macro (IEEE Cat No. 04EX821)*, Apr. 2004, pp. 1223–1226 Vol. 2. [Online]. Available: <https://ieeexplore.ieee.org/abstract/document/1398765>
- [43] T. Le, R. Chartrand, and T. J. Asaki, "A Variational Approach to Reconstructing Images Corrupted by Poisson Noise," *Journal of Mathematical Imaging and Vision*, vol. 27, no. 3, pp. 257–263, Apr. 2007. [Online]. Available: <https://doi.org/10.1007/s10851-007-0652-y>
- [44] V. B. S. Prasath, "Quantum Noise Removal in X-Ray Images with Adaptive Total Variation Regularization," *Informatica*, vol. 28, no. 3, pp. 505–515, Jan. 2017, publisher: Vilnius University Institute of Data Science and Digital Technologies. [Online]. Available: <https://informatica.vu.lt/journal/INFORMATICA/article/859>
- [45] H. Liu, Z. Zhang, L. Xiao, and Z. Wei, "Poisson noise removal based on nonlocal total variation with Euler's elastica pre-processing," *Journal of Shanghai Jiaotong University (Science)*, vol. 22, no. 5, pp. 609–614, Oct. 2017. [Online]. Available: <https://doi.org/10.1007/s12204-017-1878-5>
- [46] M. Mahmoudi and G. Sapiro, "Fast image and video denoising via nonlocal means of similar neighborhoods," *IEEE Signal Processing Letters*, vol. 12, no. 12, pp. 839–842, 2005.
- [47] P. Coupé, P. Yger, and C. Barillot, "Fast Non Local Means Denoising for 3D MR Images," in *Medical Image Computing and Computer-Assisted Intervention – MICCAI 2006*, R. Larsen, M. Nielsen, and J. Sporring, Eds. Berlin, Heidelberg: Springer, 2006, pp. 33–40.

- [48] C.-A. Deledalle, F. Tupin, and L. Denis, "Poisson nl means: Unsupervised non local means for poisson noise," in *2010 IEEE International Conference on Image Processing*, 2010, pp. 801–804.
- [49] J. Shim, M. Yoon, and Y. Lee, "Feasibility of newly designed fast non local means (FNLN)-based noise reduction filter for X-ray imaging: A simulation study," *Optik*, vol. 160, pp. 124–130, May 2018. [Online]. Available: <https://www.sciencedirect.com/science/article/pii/S0030402618301207>
- [50] "The Wiener filter." [Online]. Available: https://homepages.inf.ed.ac.uk/rbf/CVonline/LOCAL_COPIES/VELDHUIZEN/node15.html
- [51] L. Wang, J. Lu, Y. Li, T. Yahagi, and T. Okamoto, "Noise removal for medical X-ray images in wavelet domain," *Electrical Engineering in Japan*, vol. 163, no. 3, pp. 37–46, 2008, eprint: <https://onlinelibrary.wiley.com/doi/pdf/10.1002/eej.20486>. [Online]. Available: <https://onlinelibrary.wiley.com/doi/abs/10.1002/eej.20486>
- [52] V. Göreke, "A novel method based on Wiener filter for denoising Poisson noise from medical X-Ray images," *Biomedical Signal Processing and Control*, vol. 79, p. 104031, Jan. 2023. [Online]. Available: <https://www.sciencedirect.com/science/article/pii/S1746809422005080>
- [53] F. Luisier, C. Vonesch, T. Blu, and M. Unser, "Fast interscale wavelet denoising of poisson-corrupted images," *Signal Processing*, vol. 90, no. 2, pp. 415–427, 2010. [Online]. Available: <https://www.sciencedirect.com/science/article/pii/S0165168409003016>
- [54] K. Timmermann and R. Nowak, "Multiscale modeling and estimation of poisson processes with application to photon-limited imaging," *IEEE Transactions on Information Theory*, vol. 45, no. 3, pp. 846–862, 1999.
- [55] B. Zhang, J. M. Fadili, and J.-L. Starck, "Wavelets, ridgelets, and curvelets for poisson noise removal," *IEEE Transactions on Image Processing*, vol. 17, no. 7, pp. 1093–1108, 2008.
- [56] S. Gupta, L. Kaur, R. Chauhan, and S. Saxena, "A wavelet based statistical approach for speckle reduction in medical ultrasound images," in *TENCON 2003. Conference on Convergent Technologies for Asia-Pacific Region*, vol. 2, 2003, pp. 534–537 Vol.2.
- [57] L. Du, Y. Wen, and J. Ma, "Dual tree complex wavelet transform and bayesian estimation based denoising of poisson-corrupted x-ray images," in *2013 Fourth International Conference on Intelligent Control and Information Processing (ICICIP)*, 2013, pp. 598–603.
- [58] M. Makitalo and A. Foi, "Optimal inversion of the generalized anscombe transformation for poisson-gaussian noise," *IEEE Transactions on Image Processing*, vol. 22, no. 1, pp. 91–103, 2013.
- [59] J. Ren, A. Cai, N. Liang, Y. Wang, X. Zhang, L. Li, and B. Yan, "A simulation study on photon-counting denoising based on subspace decomposition," in

- 5th International Conference on Information Science, Electrical, and Automation Engineering (ISEAE 2023)*, vol. 12748. SPIE, Aug. 2023, pp. 80–86. [Online]. Available: <https://www.spiedigitallibrary.org/conference-proceedings-of-spie/12748/127480E/A-simulation-study-on-photon-counting-denoising-based-on-subspace/10.1117/12.2689447.full>
- [60] J. Salmon, Z. Harmany, C.-A. Deledalle, and R. Willett, “Poisson noise reduction with non-local pca,” *Journal of mathematical imaging and vision*, vol. 48, pp. 279–294, 2014.
- [61] W. Feng, H. Qiao, and Y. Chen, “Poisson noise reduction with higher-order natural image prior model,” *SIAM Journal on Imaging Sciences*, vol. 9, no. 3, pp. 1502–1524, 2016. [Online]. Available: <https://doi.org/10.1137/16M1072930>
- [62] J. Jisha and V. Sureshkumar, “Poisson noise removal in biomedical images using non-linear techniques,” *International Journal of Advanced Research in Electrical, Electronics and Instrumentation Engineering*, vol. 3, pp. 131–136, 2014.
- [63] K. Dabov, A. Foi, V. Katkovnik, and K. Egiazarian, “Image denoising by sparse 3-d transform-domain collaborative filtering,” *IEEE Transactions on Image Processing*, vol. 16, no. 8, pp. 2080–2095, 2007.
- [64] K. He, J. Sun, and X. Tang, “Guided image filtering,” *IEEE Transactions on Pattern Analysis and Machine Intelligence*, vol. 35, no. 6, pp. 1397–1409, 2013.
- [65] G. Treece, “The bitonic filter: Linear filtering in an edge-preserving morphological framework,” *IEEE Transactions on Image Processing*, vol. 25, no. 11, pp. 5199–5211, 2016.
- [66] S. G. Hariharan, C. Kaethner, N. Strobel, M. Kowarschik, S. Albarqouni, R. Fahrig, and N. Navab, “Learning-Based X-Ray Image Denoising Utilizing Model-Based Image Simulations,” in *Medical Image Computing and Computer Assisted Intervention – MICCAI 2019*, D. Shen, T. Liu, T. M. Peters, L. H. Staib, C. Essert, S. Zhou, P.-T. Yap, and A. Khan, Eds. Cham: Springer International Publishing, 2019, pp. 549–557.
- [67] R. Nadkarni, D. P. Clark, A. J. Allphin, and C. T. Badea, “A Deep Learning Approach for Rapid and Generalizable Denoising of Photon-Counting Micro-CT Images,” *Tomography*, vol. 9, no. 4, pp. 1286–1302, Aug. 2023, number: 4 Publisher: Multidisciplinary Digital Publishing Institute. [Online]. Available: <https://www.mdpi.com/2379-139X/9/4/102>
- [68] J. Lehtinen, J. Munkberg, J. Hasselgren, S. Laine, T. Karras, M. Aittala, and T. Aila, “Noise2Noise: Learning image restoration without clean data,” in *Proceedings of the 35th International Conference on Machine Learning*, ser. Proceedings of Machine Learning Research, J. Dy and A. Krause, Eds., vol. 80. PMLR, 10–15 Jul 2018, pp. 2965–2974. [Online]. Available: <https://proceedings.mlr.press/v80/lehtinen18a.html>

- [69] S. Wang, Z. Su, L. Ying, X. Peng, S. Zhu, F. Liang, D. Feng, and D. Liang, “Accelerating magnetic resonance imaging via deep learning,” in *2016 IEEE 13th international symposium on biomedical imaging (ISBI)*. IEEE, 2016, pp. 514–517.
- [70] D. Lee, J. Yoo, and J. C. Ye, “Deep residual learning for compressed sensing mri,” in *2017 IEEE 14th International Symposium on Biomedical Imaging (ISBI 2017)*, 2017, pp. 15–18.
- [71] A. Krull, T.-O. Buchholz, and F. Jug, “Noise2void - learning denoising from single noisy images,” in *2019 IEEE/CVF Conference on Computer Vision and Pattern Recognition (CVPR)*, 2019, pp. 2124–2132.
- [72] K. Zhang, W. Zuo, Y. Chen, D. Meng, and L. Zhang, “Beyond a gaussian denoiser: Residual learning of deep cnn for image denoising,” *IEEE Transactions on Image Processing*, vol. 26, no. 7, pp. 3142–3155, 2017.
- [73] S. Chang, J. F. M. Jr, E. K. Koons, H. Gong, C. H. McCollough, and S. Leng, “Improved noise reduction in photon-counting detector CT using prior knowledge-aware iterative denoising neural network,” *Journal of Medical Imaging*, vol. 11, no. S1, p. S12804, May 2024, publisher: SPIE. [Online]. Available: <https://www.spiedigitallibrary.org/journals/journal-of-medical-imaging/volume-11/issue-S1/S12804/Improved-noise-reduction-in-photon-counting-detector-CT-using-prior/10.1117/1.JMI.11.S1.S12804.full>
- [74] F. I. Baffour, N. R. Huber, A. Ferrero, K. Rajendran, K. N. Glazebrook, N. B. Larson, S. Kumar, J. M. Cook, S. Leng, E. R. Shanblatt, C. H. McCollough, and J. G. Fletcher, “Photon-counting Detector CT with Deep Learning Noise Reduction to Detect Multiple Myeloma,” *Radiology*, vol. 306, no. 1, pp. 229–236, Jan. 2023, publisher: Radiological Society of North America. [Online]. Available: <https://pubs.rsna.org/doi/full/10.1148/radiol.220311>
- [75] N. Ducros, J. F. P.-J. Abascal, B. Sixou, S. Rit, and F. Peyrin, “Regularization of nonlinear decomposition of spectral x-ray projection images,” *Medical physics*, vol. 44, no. 9, pp. e174–e187, 2017.
- [76] W. Zhang, N. Liang, Z. Wang, A. Cai, L. Wang, C. Tang, Z. Zheng, L. Li, B. Yan, and G. Hu, “Multi-energy ct reconstruction using tensor nonlocal similarity and spatial sparsity regularization,” *Quantitative Imaging in Medicine and Surgery*, vol. 10, no. 10, p. 1940, 2020.
- [77] W. Sun, B. Cui, Z. Lan, L. Li, X. Tang, X. Zhang, J. Ren, N. Liang, L. Lei, and Y. Bin, “Research on noise reduction technology of PCD spectral imaging based on Transformer,” in *Proceedings of the 4th International Conference on Artificial Intelligence and Computer Engineering*, ser. ICAICE '23. New York, NY, USA: Association for Computing Machinery, May 2024, pp. 286–290. [Online]. Available: <https://dl.acm.org/doi/10.1145/3652628.3652675>

Appendix A

Supporting Data

Appendix B

Satirical Support